

## Hazard Surveillance for Industrial Magnetic Fields: II. Field Characteristics from Waveform Measurements

J. D. BOWMAN\* and M. M. METHNER

National Institute for Occupational Safety and Health (Mail Stop C-27), 4676 Columbia Parkway,  
Cincinnati, OH 45226, USA

Magnetic field characteristics have been surveyed systematically in six factories with the Multiwave® II waveform capture instrument. These six facilities manufactured plastics, pharmaceuticals, cement, liquid air products, aluminum parts, and aluminum-framed filters. The study goals were to survey the physical characteristics of magnetic fields that may be related to biological effects under various interaction mechanisms and to relate those characteristics to the field's sources. From 59 waveform measurements at worker locations near sources, we calculated the extremely low frequency (ELF) and static field magnitudes, their frequency characteristics, and spatial characteristics of the 60 Hz component. The RMS vector magnitude of the ELF magnetic field (the usual exposure metric in most studies) had medians ranging from 0.53 to 12.83  $\mu\text{T}$  in the six factories. The static magnetic field magnitudes had medians of 24.2–46.2  $\mu\text{T}$ , which is well below the geomagnetic reference field of 55.0  $\mu\text{T}$  because of shielding from steel structures. The maximum static field was 128.6  $\mu\text{T}$  near a DC motor. The frequency spectra of the most common fields is dominated by 60 Hz, and has a median total harmonic distortion equal to 14.8%. The most common higher frequencies are the third, fifth, and second harmonics of 60 Hz. However, magnetic fields in these workplaces had many other 60 Hz harmonics and non-harmonic frequencies due particularly to electric motors and computer monitors. The 60 Hz component magnetic fields have elliptical polarization with median axial ratio of 25.4%. The average proportion of the 60 Hz component parallel to the static field vector was  $51.5 \pm 3.0\%$ , which indicates a significant trend towards perpendicular orientation between these two field components. In this survey of only six factories, the Multiwave® II measurements documented a wide diversity of complex magnetic field characteristics and non-sinusoidal waveforms. Although these characteristics are important to the various mechanisms postulated to explain biological effects, they are overlooked by the popular exposure assessment methods which only measure the ELF magnitude. Therefore, spot measurements with the Multiwave® II or similar waveform capture instruments are necessary for a complete magnetic field exposure assessment. Published by Elsevier Science Ltd on behalf of British Occupational Hygiene Society.

**Keywords:** EMF; extremely low frequency; ELF; exposure assessment; waveform; cancer; neurodegenerative diseases

### INTRODUCTION

Workplace magnetic fields present an unusual challenge for hazard surveillance because of their physical complexity and uncertainty about their health effects (Portier and Wolfe, 1998). The magnetic field

vector in workplaces traces out a complicated shape over time (Fig. 1). At different magnetic field sources, these vector traces vary widely in magnitude, frequency content, shape, and other field characteristics. Which of these magnetic field characteristics should be measured in research studies or health hazard evaluations has been intensely studied and debated (Valberg *et al.*, 1995; McKinlay and Repacholi, 1999; Bowman *et al.*, 2000).

In selecting exposure metrics to measure, this hazard surveillance of workplace magnetic fields used

Received 12 April 1999; in final form 19 January 2000  
\*Author to whom correspondence should be addressed. Tel.: +1-513-533-8143; fax: +1-513-533-8510; e-mail: jdb0@cdc.gov

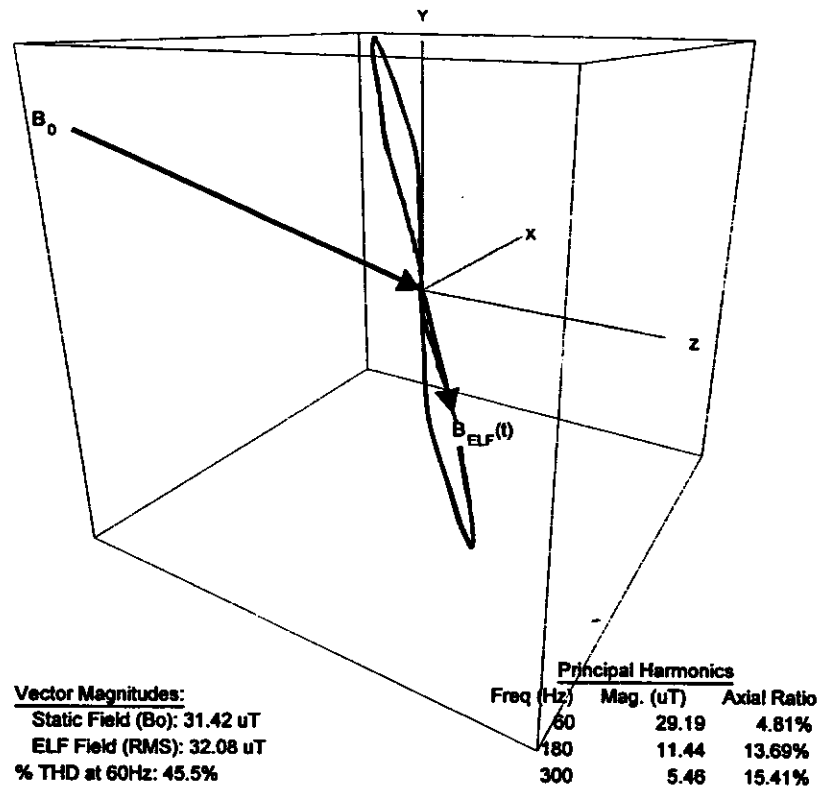


Fig. 1. The static magnetic field vector  $B_0$  and the trace of the extremely low-frequency field vector  $B_{\text{ELF}}(t)$  measured by the Multiwave II for five 60 Hz cycles (83.35 ms). The measurement was taken near a transformer in a liquid air separation plant.

two strategies. In Part I (Methner and Bowman, 2000), the exposure metric is the conventional choice for most health studies: the root-mean-square (RMS) magnitude of the magnetic field vector at extremely low frequencies (ELF = 3–3000 Hz). This exposure metric is conveniently measured by the EMDEX and other magnetic field monitors, and has been the basis for most occupational epidemiologic studies with measured EMF exposures (Portier and Wolfe, 1998, Chapter 2). Because of significant associations between the time-averaged ELF magnetic field magnitude and chronic lymphocytic leukemia in some studies, occupational ELF-EMF has been classified as a 'possible carcinogen', yet there remains much unexplained variation in the risk estimates (Portier and Wolfe, 1998, Chapter 4.2).

One possible explanation for inconsistent epidemiologic findings is that other EMF characteristics besides the RMS magnetic field magnitude may affect biological systems (NIEHS, 1997; Bowman *et al.*, 2000). Based on laboratory studies, researchers have proposed several biophysical mechanisms for EMF interactions which involve other field characteristics:

- internal electrical fields induced by external electric fields and  $dB/dt$  (NIEHS, 1997);
- induced electric fields from high-frequency transients (Sastre *et al.*, 2000);

- free radical mechanisms which respond to the total magnetic field (ELF and static) (Walleczek, 1995; NIEHS, 1997);
- ion parametric resonances that are a function of the static magnetic field magnitude, the oscillating field's magnitude, their relative spatial orientation, and the frequency spectrum (Blanchard and Blackman, 1994; Lednev, 1994; NIEHS, 1997);
- temporal coherence (Litovitz *et al.*, 1997).

These biophysical mechanisms have only been studied in theoretical and laboratory models, so their contributions (if any) to the etiology of cancer or other diseases is not yet established. However, all these mechanisms suggest that other EMF characteristics beyond the time-averaged ELF magnetic field magnitude should be involved in any association with disease. One goal of this survey is to measure as many of these characteristics as possible with one instrument as a foundation for improved exposure assessments in future health studies.

In Part II of the EMF hazard surveillance, many of these biologically relevant magnetic field characteristics were measured by a waveform capture instrument, the Multiwave® System II (Electric Research and Management, Inc., State College, PA). The Multiwave II has a three-axis fluxgate magnetometer probe, which can measure both the static magnetic

field (0 Hz) and ELF fields up to 3000 Hz. The three-dimensional waveform measurements are digitized and put through a Fast Fourier Transform (FFT) to obtain frequency spectra. From the FFT, the Multiwave's software calculates and graphs many magnetic field characteristics (Dietrich *et al.*, 1992).

For this study, spot measurements with the Multiwave II were taken during six of the walkthrough surveys at industrial facilities described in Part I. These field characteristics were also related to the electrical properties of magnetic field sources recorded during the walkthrough.

### METHODS

For Part I of the hazard surveillance, walkthrough surveys were performed in 62 facilities selected from industries with high electrical consumption (Methner and Bowman, 2000). Since the 4.5 kg Multiwave II required a second person to carry and operate, the waveform measurements were only taken at a subset of six facilities (10%) in the hazard surveillance (Table 1).

The Multiwave operator accompanied the EMDEX operator during the walkthrough survey, and took spot measurements at work stations where workers spent long periods of time near magnetic field sources. The Multiwave operator placed the probe mounted on a one-meter tall stand as close as possible to an individual's work station (within 0.3 m). A single measurement was taken at each source.

The Multiwave was configured prior to the survey so that all spot measurements consisted of 512 data points per axis (the 'A/D count') recorded at a sampling frequency of 6142.5 Hz (the 'A/D rate'). With this configuration, the waveform's duration is 83.35 ms, which encompasses five 60 Hz cycles. The frequency spectra have a base frequency of 12 Hz and go up to 3000 Hz, the cut-point of the anti-aliasing low-pass filter in the Multiwave hardware. The 12 Hz base frequency was chosen because it is a common factor of both 60 Hz from AC electricity in the United States and 72 Hz from computer monitors.

Once the waveform was captured, the second operator put the EMDEX in the same place occupied by the Multiwave probe and recorded the measurement after the instrument's read-out had stabilized. At each

site, we also noted the time, primary work process, and any specifications available for electrical equipment (for example 10 HP electric motor-3 phase-5 A). After the walkthrough, the Multiwave data were downloaded onto pre-labeled floppy disks.

In the analysis stage, the measurements were first reviewed for data quality with Multiwave's QuickPlot program, which displays waveforms, frequency spectra, and the ELF vector as a function of measurement time. In addition, we used ERM's Analysis program to make data sets with the sample time, ELF magnitude, primary frequency, and flags for out-of-range samples. With these tools, we reviewed all Multiwave measurements, and identified those that were problematic because:

1. the field exceeded the probe's limits;
2. the baseline shifted; or
3. the primary frequency was not an integer multiple of the base frequency.

This was all entered onto a spreadsheet, along with the EMDEX magnitudes, sample times, and source specifications.

From this data review, only one of 59 measurements was out-of-range (due to a high static magnetic field from an aluminum anodizing tank). However, a large proportion of the waveforms displayed shifts in the baseline (Fig. 2) caused by the probe moving through gradients in the static magnetic field near steel objects. Since probe motion from uneven floors or vibrations creates artifacts in digital Fourier transforms (Fig. 3), a new algorithm was developed to flatten the baseline (Fig. 2) and remove the FFT artifacts (Fig. 3). For this FFT correction algorithm (Gish *et al.*, 1995), we used the 12 Hz subharmonic as the indicator of probe motion, and applied these corrections to all measurements in the primary data analysis.

The qualitative review also identified waveforms that did not have an integral number of cycles in the sampling window. Since these waveforms contain frequencies that are not multiples of the base frequency, the FFT has broad bands centered on the multiple of 12 Hz that most closely approximates the true frequency. To obtain the true principal frequency, we measured the time span  $\Delta t$  between  $N$  peaks in the waveform, and calculated  $f = N/\Delta t$ .

Magnetic field characteristics were calculated by

Table 1. Facilities in the Multiwave survey

Process description	SIC (four-digit)	Area (m <sup>2</sup> )	Monthly power usage (kW-h)
Preparation of aluminum-framed filters	2621	5600	6000
Liquid air separation plant (N <sub>2</sub> , O <sub>2</sub> , Ar)	2813	9300	10 000 000
Convert plastic monomers into polymers (extrusion process)	2821	13 100	135 000
Pharmaceutical manufacturing (oral drug delivery)	2834	1800	62 000
Excavate and crush rock, produce cement powder	3241	27 900	5 000 000
Custom aluminum extruder and anodizer	3334	7400	25 000

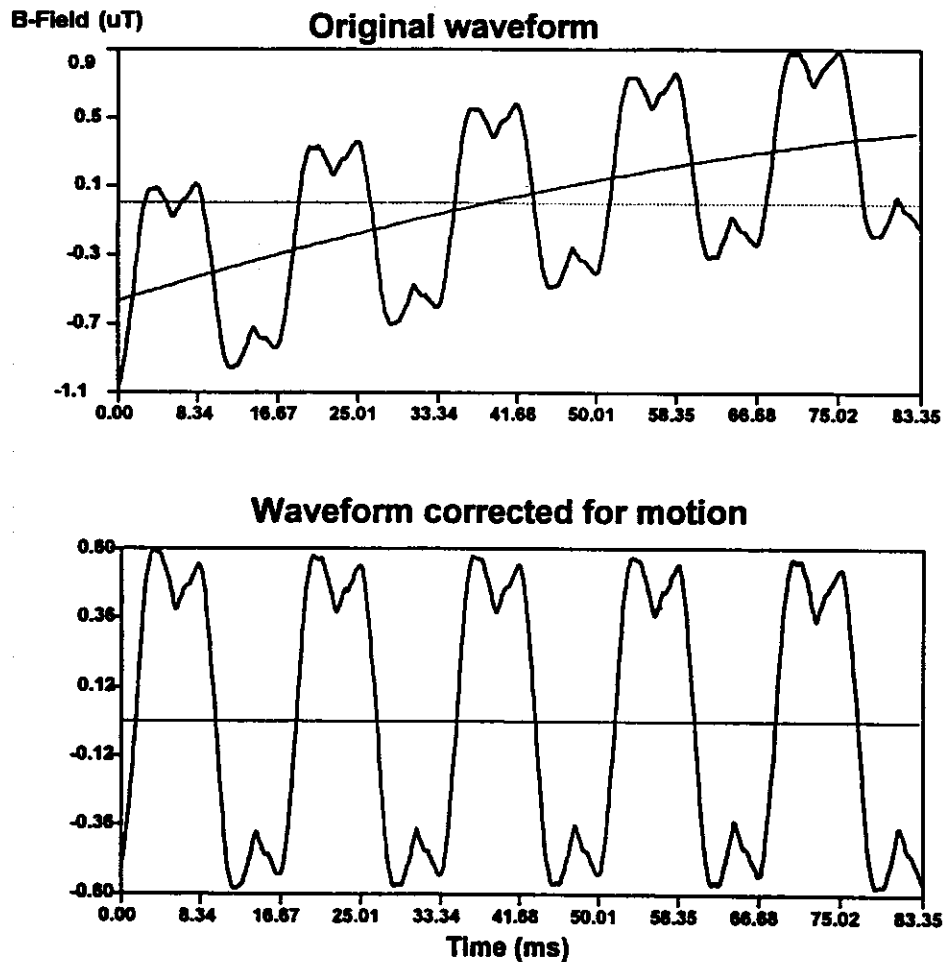


Fig. 2. Waveform measured with a moving probe: (a) the original measurement and (b) the waveform after processing with the motion correction algorithm.

the Multiwave's Analysis program (ERM, 1997) after all out-of-range waveforms were removed. We calculated the following characteristics for this survey:

- rms vector magnitude of the ELF field ( $B_{ELF}$ );
- static field magnitude ( $B_0$ );
- total harmonic distortion (THD) relative to 60 Hz (that is the combined magnitude of all harmonics of 60 Hz divided by the 60 Hz magnitude);
- rms magnitudes for 60 Hz and its harmonics up to 360 Hz;
- primary frequency (that is the frequency with the greatest magnitude);
- 60 Hz magnitude parallel to the static field vector  $B_0$  ( $B_{\parallel}$ );
- 60 Hz magnitude perpendicular to  $B_0$  ( $B_{\perp}$ );
- the axial ratio at 60 Hz (that is the ratio of the minor axis to the major axis from the ellipse traced by a sinusoidal magnetic field with a single frequency).

Mathematical definitions of these characteristics are given in Bowman (1998).

The Analysis program was also run with digital filters for the EMDEX's broadband and harmonic modes (Fig. 4) in order to calculate RMS vector magnitudes that can be compared with the concurrent EMDEX-II measurements. Summary statistics for these field characteristics were calculated for all measurements and for individual facilities.

To supplement the quantitative analysis of the field characteristics, waveforms with unusual harmonics or non-harmonic frequencies were printed out for further study and comparison with the source data. In addition, we developed new graphics software to plot three-dimensional traces of the magnetic field vectors over time (Fig. 1).

## RESULTS

The Multiwave surveillance was conducted at six manufacturing facilities, or 10% of the plants in the EMF hazard surveillance. Table 1 summarizes the six facilities surveyed, their primary products, Standard Industrial Classification (SIC), and other statistics. At

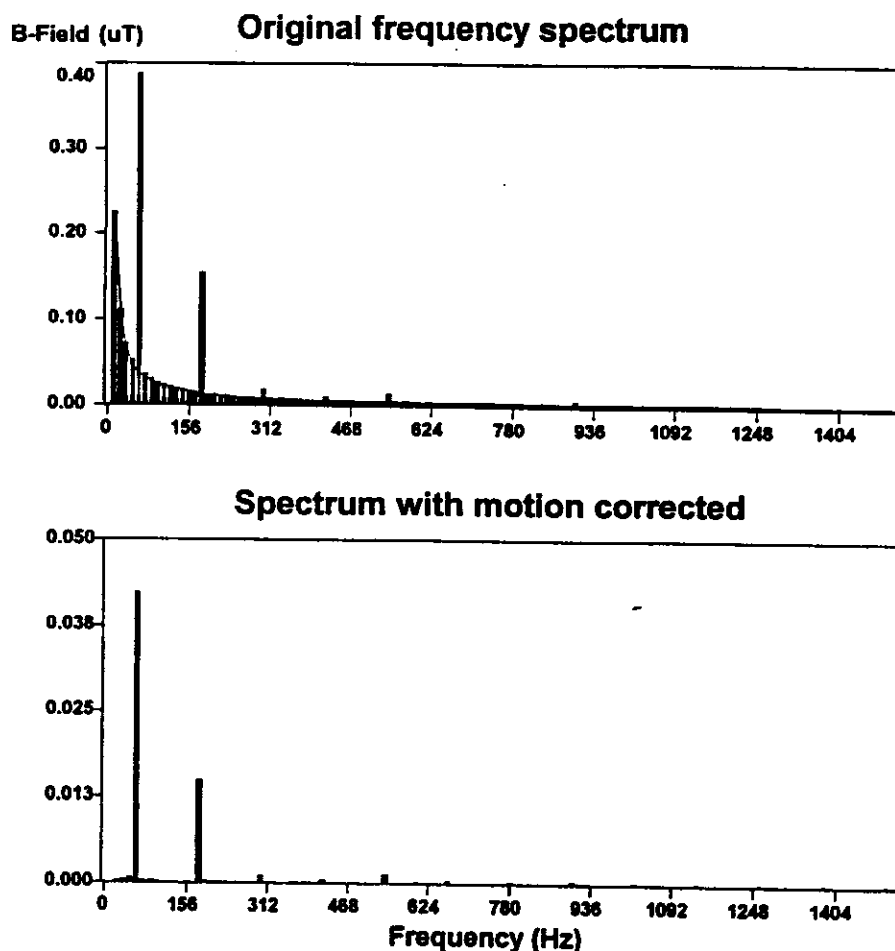


Fig. 3. Effect of the motion correction algorithm on the frequency spectrum: (a) spectrum calculated from waveform in Fig. 2 and (b) spectrum after motion correction.

each facility, 7–12 Multiwave measurements were taken, giving a total of 59 valid measurements. Four basic field characteristics from all the measurements are listed in Table 2 in order of increasing ELF magnitudes, along with their sources: 24 electric motors, 8 power supply devices, 5 heaters, 6 control devices, and 16 other kinds of machinery.

Summary statistics for all field characteristics are given in Table 3 for the total data set. For nearly all metrics, the mean is greater than the median, and less than the standard deviation, indicating that the distributions are skewed towards higher values. For most metrics, the geometric mean is approximately equal to the median, indicating a log-normal distribution. However, this generalization does not hold in some important cases (for example the geometric mean of the ELF magnitude is greater than the median). Therefore, the field characteristics for the different facilities are most reliably summarized by non-parametric statistics—the median for the central tendency (Table 4) and the range for the spread in the distribution (Table 5).

The medians in Table 5 express the characteristics of the 'common' magnetic fields at work locations near visible sources in these manufacturing facilities. Common fields like the one illustrated in Fig. 1 and Table 5 generally arise from electrical currents with the 60 Hz power frequency, either in power supplies or simple electrical circuits such as those in resistance heaters or AC motors. From this survey, some generalizations can be made about the common AC magnetic fields in manufacturing plants.

#### *ELF magnitudes*

The median ELF magnitude from all measurements in these six plants was 1.10 µT, and varied from 0.59 to 12.83 µT between the plants (Table 3). As determined with EMDEX measurements, the ELF magnitudes are not a function of the two-digit Standard Industrial Classifications (Methner and Bowman, 2000). Also the median magnetic fields and the facility's power consumption (Table 1) correlate weakly (Spearman correlation = 0.371).

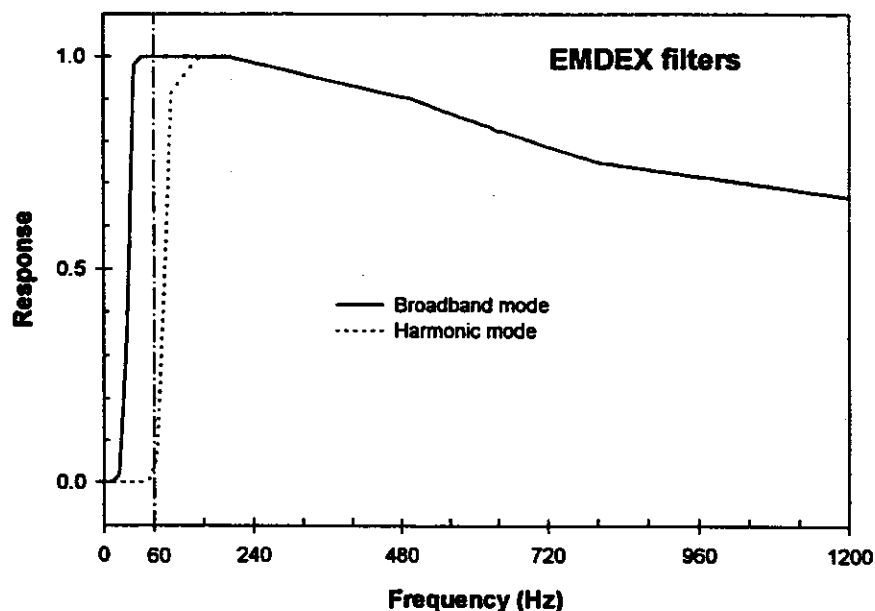


Fig. 4. Digital filters for Multiwave analyses which emulate the broadband and harmonic response modes of the EMDEX-II.

#### Static magnitudes

The median static field was  $39.24 \mu\text{T}$  for all measurements. The medians by facility fell into two groups— $<30 \mu\text{T}$  for the liquid air and drug plants, and  $>40 \mu\text{T}$  for the others (Table 4). The static field is generally the geomagnetic field perturbed by steel in the vicinity. The median measurements are well below the  $55 \mu\text{T}$  geomagnetic reference field for Ohio where the surveys took place (National Geophysical Data Center, 1998). Therefore, steel structures and machinery are generally shielding work locations from the earth's magnetic field, especially in the liquid air and drug plants.

#### Polarization

The 60 Hz component of the field has elliptical polarization with a median axial ratio of 25.4% for all measurements, which was substantially different only at the aluminum parts plant (median = 34.3%). The 'polarization' of all frequencies combined can also be studied by examining the shape of the vector traces (Tables 6–9). The complex shapes of the vector traces come from the superposition of elliptical traces at the different frequencies in the field's spectrum. Even the frequency combination of 60, 180, and 300 Hz, which is typical of 60 Hz electricity, displays a wide variety of shapes (Fig. 1 and Table 6). This overall polarization of the magnetic field is quantified by the spectrum of frequency-specific axial ratios for the principal harmonics (Fig. 1, and Tables 6–9). Small axial ratios for the principal harmonic mean thin traces approaching linear polarization (for example Fig. 1), while larger axial ratios result in more elliptical traces (for example Table 9). The origin of magnetic field

polarizations has been systematically studied for high-voltage power lines (Deno, 1976) but not for industrial sources like these.

#### AC/DC orientation

The percentage of the 60 Hz field parallel to the static field vector had a median of 51.4% for all measurements (Table 3). In the six factories, the median parallel component ranges from 29.5% in the filter plant to 67.6% in the cement plant (Table 4).

An interesting question is whether parallel or perpendicular orientations between  $B_0$  and  $B_{60}(t)$  are preferred because the sources of the two fields are related. In most cases,  $B_0$  is the geomagnetic field perturbed by steel objects in the environment, and would presumably have no connection to fields from electricity at the 60 Hz power frequency. Only when 60 Hz and DC currents are present in the same source (like a DC motor) would these two fields have some preferred alignment. This *spatial anisotropy* between  $B_0$  and  $B_{60}(t)$  is measured by the proportion of the 60 Hz vector parallel to the static vector:

$$\% \gamma = 100\% \frac{B_{\parallel}}{B_{60}} = 100\% \frac{B_{\parallel}}{\sqrt{B_{\parallel}^2 + B_{\perp}^2}} \quad (1)$$

where  $B_{\parallel}$  and  $B_{\perp}$  are the parallel and perpendicular components of  $B_{60}$ .

For a statistical test of the orientation between the 60 Hz and static fields, the null hypothesis is zero correlation between the two vectors (*spatial isotropy*), implying that  $B_{\parallel}$  is on average as likely as each of the two perpendicular components:

Table 2. Basic magnetic field metrics from the Multiwave spot measurement at each source in the six industrial facilities (with Standard Industrial Codes)

Source	ELF magnitude ( $\mu$ T)	Static field magnitude ( $\mu$ T)	THD at 60 Hz	Principal frequency (Hz)
Aluminum-framed filter plant (SIC 2621)				
Heat sealer	0.08	55.14	63.7%	60
Heat shrinker	0.13	46.17	14.8%	60
Electrical panel near work station	0.16	40.19	21.0%	60
Roll former	0.37	59.25	31.4%	60
Hand turndown motor	0.43	52.99	6.6%	60
Electrical panel near work station	0.59	43.89	33.6%	60
Fit line cut-off	0.65	55.32	12.8%	60
Electrical panel near work station	0.81	44.21	32.9%	60
Charcoal oven power supply	2.03	19.69	2.7%	60
DC forklift	2.21	24.87	322.4%	168
2 HP DC motor	4.04	128.58	2660.7%	120
Liquid air separation plant (SIC 2813)				
Control panel work station	0.09	24.19	25.3%	60
Chart recorder	1.18	22.56	23.5%	60
Cooling water pump motor	2.94	72.49	65.7%	60
LAC induction motor	6.60	21.48	1.4%	60
Compressor motor	9.06	23.57	1.5%	60
Compressor motor	12.83	40.02	3.2%	60
3500 HP motor	17.95	53.56	2.4%	60
DC battery charger	24.20	22.13	1.7%	60
Compressor motor	27.84	26.62	16.1%	60
Transformer	32.08	31.42	45.5%	60
Glove warmer	77.31	12.70	45.8%	60
Plastics plant (SIC 2821)				
Banbury control room	0.16	21.32	37.8%	60
Extruder line	0.23	47.73	37.4%	72
Blender control room	0.26	25.52	15.9%	60
Extruder operator station number 2	0.38	43.26	70.3%	60
Extruder operator station	0.53	45.69	30.0%	60
Mill roll operator station	0.94	56.26	323.6%	360
200 HP motor power line	1.87	26.78	7.1%	60
Substation	17.49	4.95	5.3%	60
Heat transfer	21.58	47.05	8.5%	60
Drug plant (SIC 2834)				
Air dryer	0.33	27.35	26.1%	60
Electronic scale control panel	0.41	39.24	39.5%	60
Electronic scale control panel	0.42	31.64	39.6%	60
Electrical panel	0.51	26.14	4.5%	60
Control panel for separator	2.29	42.37	18.0%	60
15 HP motor on boiler	2.49	45.83	5.8%	60
10 HP induction motor	3.01	28.23	1.9%	60
15 HP motor	3.86	32.92	2.5%	60
Air compressor motor	5.84	24.75	3.2%	60
800 A switchgear	37.09	8.75	2.6%	60
Cement plant (SIC 3241)				
Lab work area	0.13	38.04	96.3%	60
Rock belt motor	0.20	122.03	9.7%	60
Cement bagging station	0.43	33.28	5.7%	60
30 HP motor	0.54	104.51	4.8%	60
Mill motor	0.74	66.64	14.8%	60
Electrostatic precipitator	0.74	41.80	105.4%	120
1500 HP motor	1.09	27.84	20.0%	60
Crusher motor	1.49	13.30	12.9%	60
Rock elevator motor	3.69	44.65	9.4%	60
200 HP induction motor	4.22	37.34	5.2%	60
Main air compressor	21.11	49.26	5.8%	60
Pump motor	22.54	39.64	13.1%	60
Aluminum parts plant (SIC 3334)				
Operator work station	0.20	20.21	3.0%	60

(Continued on next page)

Table 2. (Continued)

Source	ELF magnitude ( $\mu\text{T}$ )	Static field magnitude ( $\mu\text{T}$ )	THD at 60 Hz	Principal frequency (Hz)
Miter saw (no load)	0.77	48.06	22.9%	60
Chop saw (no load)	0.84	56.84	8.6%	60
Radial arm saw (no load)	1.10	54.77	33.7%	60
DC motor	2.81	34.12	16.3%	60
Air compressor	19.82	19.98	5.8%	60
7000 A anodizing tank	Out of range			

$B_x = \sqrt{B_x^2 + B_y^2}$ . The mean of  $\% \gamma$  from an isotropic distribution can be derived by equalizing all three vector components of  $B_{60}$  in Eq. (1), which gives:  $\% \gamma_{iso} = 100\%/\sqrt{3} = 57.7\%$ . Therefore, a means test can determine whether the average  $\% \gamma$  in a workplace shows spatial isotropy. The test statistic is:

$$t = \frac{(\% \gamma - \% \gamma_{iso}) \sqrt{n}}{s_\gamma}$$

where  $s_\gamma$  is the standard deviation of  $\% \gamma$  and  $n$  is the number of measurements (Rosner, 1995).

For all Multiwave measurements, the mean  $\% \gamma$  is  $51.5 \pm 3.0\%$ , which is significantly smaller than the  $57.7\%$  value for spatial isotropy ( $P = 0.04$ ). For five of the six individual facilities (Table 4), the percentage parallel to  $B_o$  was not significantly different from spatial isotropy, as expected. The exception was the filter plant, where the mean  $\% \gamma = 35.0 \pm 7.0\%$  is significantly anisotropic ( $P = 0.009$ ). Contrary to our prediction, this anisotropy in the filter plant was due to AC equipment where the 60 Hz component is nearly perpendicular to  $B_o$  (for example the AC control panel in Table 7). It is difficult to explain this significant preference for a perpendicular AC/DC orientation, which may be due to some regularity in the steel near 60 Hz sources in that one facility. In another surprise, three strong DC sources with  $B_o > 100 \mu\text{T}$  had an average alignment close to the isotropic value (mean  $\% \gamma = 55.1 \pm 13.9\%$ ). Clearly, the relative orientation of 60 Hz and static fields cannot be easily predicted from the presence or absence of DC currents. At most facilities in this survey, however, the spatial orientation was isotropic on average as predicted.

#### Frequency spectrum

Of the 59 measurements, 55 (that is 93%) had 60 Hz as their primary frequency in the ELF range, which is obviously due to AC electricity. The median for the total harmonic distortion was 14.8% for all facilities and varied from 5.1 to 30.0% for the individual plants. The leading harmonics expressed as a percentage of the 60 Hz magnitude are the third harmonic (median=8.2% for all facilities), the fifth

(3.1%) and the second (2.3%). The frequency content varies dramatically between facilities. The third and fifth harmonics dominated the spectrum in the liquid air plant, but the second and higher harmonics played significant roles in the other facilities, especially the plastics plant. Table 7 gives examples of waveforms with unusual harmonics in different plants.

These features of the ELF frequency spectra are explained by electrical engineering principles. As a rule, the third and fifth harmonics are most common in magnetic fields from electrical power (Table 6). The third harmonic is developed largely by the saturation characteristics of transformers throughout electrical distribution systems. The fifth and seventh are also common because the distribution system can accentuate these harmonics through resonances with the capacitor installations used for voltage control. Three-phase distribution systems tend to eliminate even harmonics because of their relatively high overall impedance and cancellation with the power frequency (an odd harmonic). Moreover, power generators cannot produce even harmonics in normal operation.

When electric power for a building is stepped down to a lower voltage, the presence of harmonics is no longer controlled by the distribution system characteristics, so many other harmonics begin to appear from local sources. For example, single-phase rectifiers produce mostly 120 Hz along with many even harmonics. The most common use of this circuit is in computer power supplies, where 120 Hz components are frequently found to be strong. This perhaps explains the fields from the extruder operator station in the plastics plant and the electrostatic precipitator in the cement plant (Table 7). In the rest of the workplace, these even harmonics from computer usage are usually diluted by larger currents going to other equipment.

The ranges for the magnetic field metrics in Table 5 indicate the diversity of fields to be found in factories. The ELF magnitude varies from 0.08 to  $77.3 \mu\text{T}$ , depending on the electric currents in the source and the distance to the measurement. Maximum ELF fields were measured near electric heaters such as the glove warmer in the liquid air plant ( $77.3 \mu\text{T}$ ) and near AC power supplies such as the 800 A switches in the pharmaceutical plant ( $37.09 \mu\text{T}$ ).



Table 3. Summary statistics of magnetic field characteristics from all Multiwave measurements in all facilities

Statistics	ELF magnitude (μT)	Static magnitude (μT)	THD at 60 Hz	Principal frequency (Hz)	60 Hz magnitude (μT)	Magnitude spectrum (percentage of magnitude)					Spatial characteristics of the 60 Hz component				
						120 Hz	180 Hz	240 Hz	300 Hz	360 Hz	Axial ratio (%)	Parallel mag. (μT)	Perp. mag. (μT)	% Parallel to B <sub>0</sub>	
N	59														
Minimum	0.08	8.8	1.4%	60	0.06	0.1%	0.8%	0.1%	0.3%	0.0%	4.8%	0.01	0.06	10.2%	
Maximum	77.31	128.6	2660.7%	360	70.28	2449.6%	262.3%	994.6%	42.2%	312.4%	77.2%	25.06	70.10	96.7%	
Mean	6.88	40.8	76.4%		6.52	51.9%	18.6%	20.2%	5.4%	13.9%	31.9%	3.43	5.92	51.4%	
Std. dev.	13.03	23.1	347.4%		12.30	318.3%	36.2%	129.2%	8.0%	53.1%	19.5%	6.03	11.60	22.8%	
Geometric mean	1.61	35.8	14.8%		1.34	3.1%	8.3%	1.0%	2.8%	0.7%	25.9%	0.61	1.22	45.5%	
Median	1.10	39.2	14.8%		0.84	2.3%	8.2%	0.7%	3.1%	0.4%	25.4%	0.48	0.75	51.1%	

Table 4. Medians of field characteristics from Multiwave measurements in each facility

Facility	N	ELF magnitude (μT)	Static magnitude (μT)	THD at 60 Hz (μT)	60 Hz magnitude (μT)	Magnitude spectrum (percentage of 60 Hz magnitude)					60 Hz spatial characteristics		
						120 Hz	180 Hz	240 Hz	300 Hz	360 Hz	Axial ratio	% Parallel to B <sub>0</sub>	P for isotropy*
Filters	11	0.59	46.2	31.4%	0.34	3.9%	16.2%	1.6%	4.0%	1.1%	24.7%	29.5%	0.01
Liquid air	11	12.83	24.2	16.1%	12.77	0.5%	15.8%	0.2%	2.6%	0.1%	25.4%	57.3%	0.69
Polymers	9	0.53	43.3	30.0%	0.31	6.5%	9.6%	4.0%	4.3%	5.3%	23.9%	51.4%	0.53
Drugs	10	2.39	29.9	5.1%	2.37	1.4%	3.3%	0.3%	1.5%	0.2%	27.4%	44.2%	0.16
Cement	12	0.91	44.1	13.5%	0.86	4.4%	7.9%	1.6%	2.4%	1.1%	25.3%	67.6%	0.13
Aluminium parts	6	0.97	41.1	12.4%	0.94	3.8%	3.3%	0.7%	2.0%	0.7%	34.3%	44.9%	0.13
All facilities	59	1.10	39.2	14.8%	0.84	2.3%	8.2%	0.7%	3.1%	0.4%	25.4%	51.1%	0.04

\*P value from t-test for the mean of %γ (percentage of 60 Hz field parallel to B<sub>0</sub>) vs %γ<sub>iso</sub>.

Table 5. Minimum and maximum of field characteristics from measurements in each facility

Facility	ELF magnitude ( $\mu\text{T}$ )	Static magnitude ( $\mu\text{T}$ )	THD at 60 Hz (%)	Principal frequency (Hz)	60 Hz magnitude ( $\mu\text{T}$ )	Magnitude spectrum (percentage of 60 Hz magnitude)					60 Hz spatial characteristics	
						120 Hz	180 Hz	240 Hz	300 Hz	360 Hz	Axial ratio %	Parallel to $B_0$
Filters	0.08	19.7	2.7%	60	0.06	0.3%	1.5%	0.1%	0.5%	0.0%	6.8%	14.3%
	4.04	128.6	2660.7%	168	2.03	2449.6%	262.3%	994.6%	42.2%	261.1%	68.7%	82.4%
Liquid air	0.09	12.7	1.4%	60	0.08	0.1%	0.8%	0.1%	0.4%	0.0%	4.8%	10.2%
	77.31	72.5	65.7%	60	70.28	44.1%	39.5%	26.2%	20.3%	23.5%	73.6%	91.0%
Polymers	0.16	15.0	5.3%	60	0.12	0.8%	1.3%	0.2%	1.6%	0.1%	6.0%	14.5%
	21.58	56.3	323.6%	360	21.49	25.2%	63.5%	11.5%	15.7%	312.4%	55.7%	79.2%
Drugs	0.33	8.8	1.9%	60	0.32	0.1%	1.5%	0.1%	0.3%	0.0%	5.8%	26.2%
	37.09	45.8	39.6%	60	37.07	17.8%	39.0%	2.3%	7.7%	1.3%	62.8%	75.7%
Cement	0.13	13.3	4.8%	60	0.09	0.8%	2.6%	0.2%	0.7%	0.2%	12.0%	37.1%
	22.54	122.0	105.4%	120	22.24	103.1%	86.7%	10.9%	38.2%	5.2%	77.2%	96.7%
Aluminum parts	0.20	20.0	3.0%	60	0.20	0.4%	1.3%	0.1%	1.2%	0.1%	9.1%	25.2%
	19.82	56.8	33.7%	60	19.79	16.0%	29.5%	12.9%	15.0%	15.5%	77.0%	65.3%
All facilities	0.08	8.8	1.4%	60	0.06	0.1%	0.8%	0.1%	0.3%	0.0%	4.8%	10.2%
	77.31	128.6	2660.7%	360	70.28	2449.6%	262.3%	994.6%	42.2%	312.4%	77.2%	96.7%



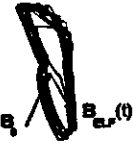
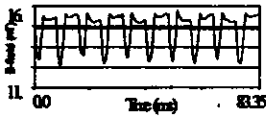
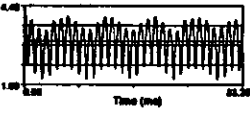

Table 6. Examples of 'common' magnetic fields

Facility Source	Drug plant Electronic scale control panel	Aluminum parts plant Radial arm saw (no load)	Liquid air separation plant Chart recorder
Vector trace (five 60 Hz cycles; $B_s$ vector not to scale)			
Waveform (one selected axis)			
Static field mag. ( $\mu$ T)	31.64	54.77	22.56
ELF magnitude ( $\mu$ T)	0.420	1.098	1.184
%THD at 60 Hz	39.5%	33.7%	23.5%
Proportion of 60 Hz parallel to $B_s$	36.3%	25.2%	64.9%
<b>Principal Harmonics</b>			
Frequency (Hz)	60    180    300	60    180    300	60    180    300
Magnitude ( $\mu$ T)	0.391   0.152   0.022	1.037   0.306   0.158	1.151   0.259   0.070
Axial ratio	25.0%   20.0%   38.7%	31.4%   26.6%   21.5%	9.8%   8.1%   15.2%

Table 7. Magnetic fields with unusual harmonics

Facility Source	Liquid air separation plant Cooling water pump motor	Cement plant Electrostatic precipitator	Filter plant AC control panel near workstation
Vector trace (five 60 Hz cycles; $B_s$ vector not to scale)			
Waveform (one selected axis)			
Static field mag. ( $\mu$ T)	12.70	41.60	44.21
ELF magnitude ( $\mu$ T)	3.042	0.741	0.829
%THD at 60 Hz	65.6%	105.4%	34.0%
Proportion of 60 Hz Parallel to $B_s$	91.0%	96.7%	35.7%
<b>Principal Harmonics</b>			
Frequency (Hz)	60    120    240	120    60    180	60    180    72
Magnitude ( $\mu$ T)	2.446   1.080   0.644	0.550   0.501   0.095	0.761   0.250   0.844
Axial ratio	20.4%   66.7%   13.9%	3.75%   25.5%   13.6%	21.3%   15.7%   23.3%

Table 8. Magnetic fields from DC motors

Facility Source	Filter plant 2 HP DC motor	Plastics plant Mill roll operator station	Filter plant DC forklift
Vector trace (five 60 Hz cycles; $B_z$ vector not to scale)			
Waveform (one selected axis)			
Static field mag. ( $\mu\text{T}$ )	128.58	56.26	24.87
ELF magnitude ( $\mu\text{T}$ )	1.354	0.937	2.237
%THD at 60 Hz	908.4%	323.8%	1440.9%
Proportion of 60 Hz Parallel to $B_z$	82.4%*	43.7%	30.1%*
Principal Harmonics			
Frequency (Hz)	120    240    360	360    60    720	168**    156**    324**
Magnitude ( $\mu\text{T}$ )	0.884    0.553    0.175	0.772    0.249    0.170	1.476    1.006    0.849
Axial ratio	53.7%    25.0%    20.8%	8.8%    8.8%    12.2%	22.8%    24.2%    33.8%

\* Statistic is unreliable because the 60 Hz component is negligible.

\*\* The FFT's harmonics are wrong because the signal's true frequencies (161.3 and 322.6 Hz) are not integer multiples of the 12 Hz base frequency.

For the static field, the minimum magnitude (8.7  $\mu\text{T}$ ) was measured within the steel shielding of the electric power switching room in the drug plant. The maximum (128.6  $\mu\text{T}$ ) occurred near a DC motor in the filter plant (Table 8).

With the THD, the lower values were generally measured near AC power supplies, but the minimum harmonic distortion (1.4 and 1.9%) were generated by induction motors. The largest THDs were greater than 100%, and occurred when 60 Hz was not the principal frequency, due to either DC electric motors or computer monitors.

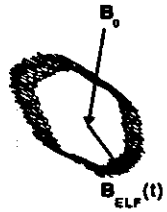
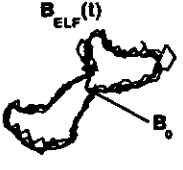
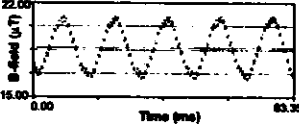
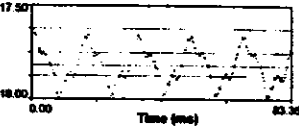
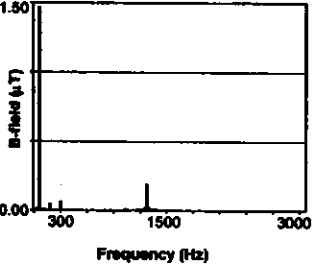
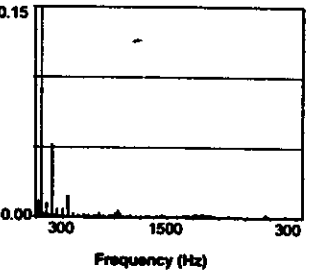
Electric motors can produce either a simple AC magnetic field (60 Hz with third and fifth harmonics, such as the radial arm saw in Table 6) or a complex array of harmonics generated by rectifiers and inverters in the electrical circuits that alter the speed of the motor (Table 8). Depending on the motor design, three-phase rectifiers tend to produce the 5th, 7th, 11th, 13th, 17th, 19th, 23rd, and 25th harmonics on the motor's AC side. The amount of each harmonic depends on the filtering in the motor's circuits. Even harmonics are seen on the DC side, which seldom has much filtering. For example, rectification with the 6th and 12th harmonics was measured at a mill roll operator station in the plastics plant (Table 8). In addition, DC motors often have high static fields as well as their ELF frequencies. For example,

the 2 HP DC motor in the filter plant with a static field of 128.6  $\mu\text{T}$  along with a 120 Hz rectified field (Table 8).

With variable-speed induction motors, the frequency need not be a multiple of 60 Hz, but is instead related to the motor's slip speed. For example, the principal frequency of the DC fork lift in the filter plant (Table 8) lies between the 156 and 168 Hz components of the FFT, and is actually 161.3 Hz when calculated from the waveform. The FFT data in Table 8 are therefore approximate. Note the forklift measurement had an unexpectedly low static field of 24.87  $\mu\text{T}$ , due perhaps to a probe location far from the DC power supply or shielding from the steel body.

Finally, we observed two electric motors with high-frequency components that could not be easily explained: a 200 HP motor in the plastics plant with 1280 Hz (Table 9) and a crusher motor in the cement plant with 1044 Hz (not shown). Without more details on the motor design, we can only speculate that these high frequencies may be caused by solid-state electronic devices for controlling the motor's speed or energy efficiency. One possibility is a tachometer that is somehow coupled to the motor's power circuits; another is a 'cyclo-converter', which alters the motor's basic frequency by switching a high-frequency carrier wave on and off at the proper times. A similar electronic device was probably responsible

Table 9. Magnetic fields with higher frequencies

Source	Power line to a 200 HP motor	Banbury mixer control room
<b>Vector trace</b> (five 60 Hz cycles; $B_0$ vector not to scale)		
<b>Waveform</b> (one selected axis)		
<b>Frequency spectrum</b>		
<b>Static field mag. (<math>\mu\text{T}</math>)</b>	26.78	21.32
<b>ELF magnitude (<math>\mu\text{T}</math>)</b>	1.873	0.161
<b>THD @ 60 Hz</b>	7.1%	38.7%
<b>Principal Harmonics</b>		
<b>Frequency (Hz)</b>	60      1272*      300	60      180      360
<b>Magnitude (<math>\mu\text{T}</math>)</b>	1.850    0.234    0.086	0.150    0.053    0.015
<b>Axial ratio</b>	45.9%    19.6%    54.6%	41.6%    88.7%    45.1%

\* This FFT harmonic is wrong because the signal's true frequency (1280.1 Hz) is not an integral multiple of the 12 Hz base frequency.

for a field with a distinct frequency of 2148 Hz and magnitude  $0.005 \mu\text{T}$ , which was measured at an AC control panel in the liquid air plant (not shown).

Higher frequency fields ( $>1000$  Hz) were occasionally detected that were probably due to electrical noise, for example the Banbury mixer control room of the plastics factory (Table 9). In contrast to fields with distinct high frequencies, the 'noisy' fields have small irregular spikes in their frequency spectra extending out as far as 3000 Hz. Since we did not observe any equipment which deliberately created sparks (for example welding, sputtering), the most likely cause of this electrical noise in the Banbury control room is therefore arcing in motors or heaters.

Another source of unusual frequencies is computer monitors, which can have vertical sweep rates of 60 and 72 Hz, among others. (The 15 kHz horizontal sweep fields are outside the Multiwave's bandwidth.)

Since the Multiwave's configuration was set so that 72 Hz is one of the FFT harmonics, we examined with our data that signature of computer monitor fields. In fact, 72 Hz was the principal frequency in field measured near an extruder line at the plastics plant (Table 2), and the  $x$ - and  $z$ -axis waveforms show some sawtooth characteristics (mixed with other harmonics) which would be expected from a video sweep current (Fig. 5). Waveforms with a 60 Hz principal frequency and the appearance of a 72 Hz sawtooth were measured at an electric panel in the drug company ( $72$  Hz magnitude equal to  $0.021 \mu\text{T}$ ) and the laboratory of the cement company ( $0.008 \mu\text{T}$ ). With other 72 Hz occurrences (for example the AC control panel in the filter plant in Table 7), it is hard to see a sawtooth, so this frequency may be noise or a motion artifact.

To study the effects of VDT fields further, Fig. 5

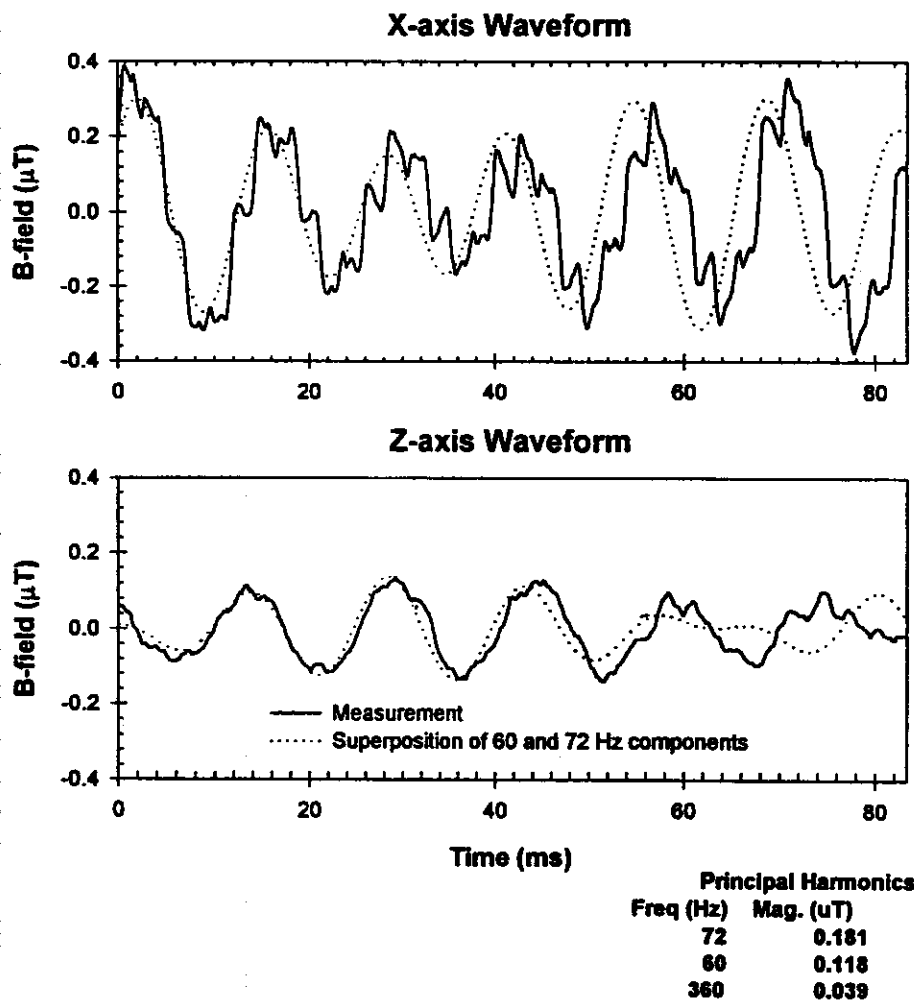


Fig. 5. Waveform measurements (solid line) which include 60 and 72 Hz components, due probably to a computer monitor. The mathematical superposition of the 60 and 72 Hz components (dotted line) shows 6 Hz beats on 66 Hz carrier waves.

also shows waveforms generated from a Fourier series with only 60 and 72 Hz components whose magnitude and phase are the FFT parameters from the plastics plant measurement (Jackson, 1991). In accordance with basic wave physics (Elmore and Heald, 1969), the superposition of these two frequencies produces 6 Hz 'beats' (half their difference) modulating a 66 Hz carrier wave (the average frequency). Mixed with the other harmonics in the spectrum, the beat pattern produces ultra-low-frequency undulations and aperiodic behavior in these unusual waveforms (Fig. 5). However, undulations and aperiodicity in a waveform can also be produced by probe motion, rapidly changing sources or other magnetic field irregularities that produce FFT artifacts. The lack of fit between the measured and modeled waveforms in Fig. 5, especially in the z-axis, suggests that the beats may be mixed with such irregularities.

The EMDEX is compared with Multiwave

measurements in Table 10. From the Multiwave measurements, the ELF magnitudes are calculated with and without a digital filter to represent the EMDEX's broadband mode (Fig. 2). When the Multiwave magnitudes passed through the EMDEX filter are compared to the simultaneous EMDEX measurements, the Spearman correlation is equal to 0.85. Although the correlation between the two instruments is highly significant ( $P < 10^{-13}$ ), the percentage difference ranges from -90 to 2325% (median=15.4%), indicating the large spatial variability in magnetic fields over the short distance between the two instruments.

The accuracy of the EMDEX filter in measuring ELF magnitudes is generally good, as indicated by the slight bias in the Multiwave measurements with and without the filter (mean error =  $-1.14 \pm 0.28\%$  in Table 10). The percentage difference is small as long as the principal frequency is 60 Hz. As the plot of the EMDEX filter in Fig. 2 suggests, measurements with

Table 10. Multiwave ELF magnitudes (unfiltered and with the EMDEX broadband filter) compared with the simultaneous EMDEX measurements

Summary statistics	Multiwave measurements			EMDEX broadband magnitude ( $\mu\text{T}$ )	% Difference between EMDEX and Multiwave (with filter)
	Unfiltered ELF magnitude ( $\mu\text{T}$ )	Magnitude with EMDEX broadband filter ( $\mu\text{T}$ )	% Difference with and without filter		
<i>N</i>	59				
Minimum	0.08	0.7	-10.78%	0.05	-90.04%
Maximum	77.31	771.5	0.00%	68.40	2325.59%
Mean	6.88	6.84	-1.14%	8.07	152.94%
Std. dev.	13.03	12.98	2.18%	13.64	404.82%
Geometric mean	1.61	1.59	n.d.*	2.52	n.d.*
Median	1.10	1.10	-0.14%	2.10	15.36%
Correlation with Multiwave (with filter)	0.999	1.000	-	0.808	-

\*No data: the geometric mean is not defined for variables  $\leq 0$ .

strong contributions from higher frequencies would have the greater biases. For example, the most extreme bias of -10.78% was measured at the mill roll operator station in the plastics plant, where the primary harmonics were 360, 60, and 720 Hz (Table 8). At these higher frequencies, EMDEX measurements become inaccurate owing to the fall-off in its filter (Fig. 2).

Finally, we calculated Spearman correlations between the ELF magnitude calculated with EMDEX's broadband filter and the other characteristics (Table 11). These correlations indicate whether a traditional exposure assessment with EMDEX-type monitors can be a surrogate for other biologically relevant exposure metrics. The only metric consistently correlated with the EMDEX magnitude was the 60 Hz magnitude ( $r = 0.93$ ). The association with the 60 Hz magnitude is weakened at the filter plant ( $r = 0.55$ ) where the DC forklift and 2 HP motor had other principal frequencies (Table 2). Significant correlations were occasionally found with harmonics of 60 Hz, especially the third and fifth harmonics, but the EMDEX was associated with different harmonics in different factories. Correlations with the static field, THD, and the spatial metrics were even weaker. The axial ratio consistently showed no correlation ( $r = 0.15$  overall). In this sample of factories, the 60 Hz magnitude was the only exposure metric that can be reliably predicted with EMDEX broadband measurements.

#### DISCUSSION

This study is one of a few exposure assessments on magnetic field characteristics in workplaces. In the previous studies, Dietrich *et al.* (1992) used the

Multiwave System with induction coil sensors in homes, electric substations, and a chemical plant; Philips *et al.* (1995) used a magnetic field spectrum analyzer with induction coil sensors and a fluxgate magnetometer in a hospital; Wenzl (1997) used the Multiwave II on electric railways; and Dietrich and Jacobs (1999) used the Multiwave System with both induction coil and fluxgate sensors in the transportation sector, including automobiles and airliners. The present study used the Multiwave II with its three-axis fluxgate probe to measure both ELF and static magnetic field characteristics reported in the previous work, and surveyed a variety of factories in industries where detailed EMF characteristics have not been measured before.

The walkthrough strategy took systematic measurements at sources near work locations throughout the factories and correlated the field characteristics with qualitative information about the sources. The number of measurements was large enough so that several hypotheses about the fields could be tested statistically. Finally, new graphics software was used to plot the vector traces, which are particularly useful for visualizing spatial characteristics. With these advantages, this Multiwave II survey has explored the characteristics of workplace magnetic fields and their relationship to sources in new depth and variety.

This survey documented both common magnetic field characteristics (Tables 4 and 6) and unusual characteristics (Tables 5, and 7-9). The most common frequency spectrum in our survey was dominated by 60 Hz and its third and fifth harmonics, a pattern also seen in homes (Dietrich *et al.*, 1992) and a hospital (Philips *et al.*, 1995). The homes and the hospital also had THDs similar to the median of 14.8% in the six factories. In contrast, the median THD was 1.4%

Table 11. Spearman correlations\* of magnetic field characteristics with the EMDEX broadband magnitude (calculated with a digital filter applied to Multiwave measurements)

Facility	Number	Static magnitude	THD at 60 Hz		Magnitude spectrum						60 Hz spatial characteristics		
			60 Hz	120 Hz	180 Hz	240 Hz	300 Hz	360 Hz	Axial ratio	Proportion parallel to $B_0$			
Filters	11	-0.14	0.23	0.35	0.81	0.25	0.79	0.26	0.21	0.58			
Liquid air	11	-0.13	0.08	0.52	0.81	0.55	0.83	0.65	-0.10	-0.18			
Plastics	9	0.08	-0.57	0.77	0.68	0.53	0.92	0.35	0.23	0.72			
Drugs	10	-0.35	-0.87	1.00	0.18	0.67	0.75	0.54	0.52	0.54			
Cement	12	-0.20	-0.16	0.98	0.80	0.85	0.80	0.75	0.20	0.41			
AI parts	6	-0.26	0.14	1.00	0.26	0.31	0.94	0.77	-0.14	-0.20			
All sites	59	-0.27	-0.39	0.93	0.62	0.73	0.62	0.58	0.15	0.40			

\*Values in bold face are different from zero with  $P < 0.05$ . Values in italic are different from zero with  $P < 0.10$ 

in electric substations and 51.3% in a chemical plant (Dietrich *et al.*, 1992). More diverse are the frequency spectra of transportation systems (Wenzl, 1997; Dietrich and Jacobs, 1999). For example, the principal frequency is 400 Hz in airliners and 25 Hz in some electrified rail lines.

For other magnetic field characteristics, the median of the axial ratio was 25.4% in our survey, which is more elliptical than in homes (mean equal to 20.3%) and substations (mean equal to 16.7%) but more linear than the chemical factory (median equal to 37.2%) (Dietrich *et al.*, 1992). The median static field magnitude of 39.2  $\mu\text{T}$  was less than the 55  $\mu\text{T}$  geomagnetic field, which Philips *et al.* (1995) also found in their hospital survey. Lastly, the percentage of the 60 Hz magnetic field parallel to the static field vector had a median of 51.1%, which is significantly less than the isotropic value of 57.7%. This spatial anisotropy metric was not measured in the previous surveys.

The wide divergence from these norms is another important result of this survey. We observed second, fourth, and sixth harmonics larger than the 60 Hz magnitude, so the THD was greater than 100% (Table 5). Dietrich *et al.* (1992) also found the maximum THD was 213% in the chemical plant. The polarization in our measurements approached linear at one extreme (minimum axial ratio equal to 4.8%) and circular at the other (maximum=77.2%). At the chemical plant, the polarization was even more circular (maximum=90.6%). In our survey, the 10.2–96.7% range in the anisotropy also approached the maximum possible extent. The static field magnitude ranged far from its norm, due to steel shielding at the minimum (8.8  $\mu\text{T}$ ) and a DC motor at the maximum (128.6  $\mu\text{T}$ ). In comparison, the static field's range was only 25.0–48.0  $\mu\text{T}$  in the hospital survey (Philips *et al.*, 1995), which resembles the range in homes (Bowman *et al.*, 1995).

The wide diversity of magnetic field characteristics in only six factories suggests that EMF in the manufacturing sector is often a heterogeneous mixture. Although the sample of factories is small and their selection opportunistic (Methner and Bowman, 2000), a larger sample would only increase the diversity of field characteristics. Measurements of the ELF magnitude cannot reliably assess the components of this mixture, outside of the 60 Hz magnitude (Table 11).

This variability of magnetic field characteristics has implications for the evaluation of the possible cancer hazards from ELF magnetic fields. Epidemiologic studies have reported significant associations of leukemia and brain cancer risks with the TWA magnitudes of workplace magnetic fields. However, occupational EMF was only rated a 'possible' carcinogen because of the lack of an established mechanism and inconsistencies between epidemiologic results (Portier and Wolfe, 1998).

The epidemiologic inconsistencies could be explained by exposure assessments that measured



only the ELF magnitude and not the other magnetic field characteristics. Inconsistency generally suggests that epidemiologic associations are not causal because differences between study results may be due to undetected confounders or other sources of bias. However, the mechanistic hypotheses listed in the Introduction suggest that some of the other EMF characteristics could be *effect modifiers*, changing the risks from the ELF magnitude observed from study to study. According to this hypothesis, inconsistencies between epidemiologic studies would be more likely in workplaces like our six factories where magnetic field characteristics vary markedly and are mostly uncorrelated with the ELF magnitude.

The diverse magnetic field characteristics observed in our survey provide further evidence that the varying risks associated with the ELF magnitude may be explained by a better assessment of occupational EMF exposures. The hypothesis that these characteristics may be effect modifiers can be tested by using waveform capture instruments like the Multiwave II to measure exposures in future epidemiologic studies. Such studies would not only clarify whether workplace EMF causes cancer, but also indicate which exposure characteristics should be measured during occupational hygiene surveys.

As a pioneering effort, our survey had weaknesses which provide lessons for future surveillance and epidemiologic studies. Since the Multiwave measurements were an adjunct to the EMDEX walkthrough survey, the small sample of facilities can not be considered representative of manufacturing plants. Taking only 6–12 Multiwave measurements at each facility was marginal for making statistical inferences between plants and too few for comparisons within a plant. Moreover, the information collected about the sources was sometimes inadequate to explain the field characteristics. In particular, the design of electric motors and the sweep rate of computer monitors (or their make and model) should be recorded systematically.

Another limitation is that the Multiwave II only responds to static and ELF magnetic fields (0–3000 Hz) with a peak amplitude of less than 500  $\mu$ T. More complete EMF surveillance would use other instruments to measure high-amplitude magnetic fields, ELF electric fields and radio frequency (RF) fields. For example, the static magnetic field from the anodizing tank at the aluminum parts plant (Table 3) exceeded the dynamic range of the Multiwave II, but could be measured with a Hall-effect probe (Bracken, 1994). Also, the heat sealer in the filter plant would probably emit 5–40 MHz electric and magnetic fields, which require an RF instrument (Conover *et al.*, 1980).

More research is needed on a systematic method for calculating accurate FFTs of workplace magnetic fields. Since the Multiwave software does all its calculations from the FFT, many (but not all the metrics)

are sensitive to an erroneous FFT. In order to prevent such errors, we set the Multiwave configuration to encompass most of the frequencies we expected in the workplace, adjusted for probe motion, and laboriously searched for artifacts. This was not always enough. Although we planned for the 72 Hz fields from Super VGA monitors in setting the Multiwave's configuration at a 12 Hz base frequency, we did not anticipate the 75 Hz sweep frequencies which other computer monitors have.

A Multiwave configuration that can encompass both kinds of monitors would have a base frequency of 3 Hz, that is the sampling window equals 333.3 ms. Since our 83 ms measurements sometimes captured variable waveforms, we had to be alert for inaccurate FFT in the interpretation of our results. Therefore, measuring four times longer would produce troublesome FFTs much more frequently. One solution would be measuring the waveform over a long 0.33 s window, but calculating the FFT only for the periodic segments of the waveform which meet the FFT criteria for the frequencies actually present. This strategy would require new software which can identify the important frequencies in the entire waveform and then 'window' the periodic segments for the accurate FFT calculation.

The motion correction algorithm also needs further research because we were not always able to correct the FFT successfully. The present algorithm cannot distinguish between irregularities in the baseline of a periodic waveform owing to probe motion and those due to variable amplitudes or frequency content over the course of the sampling window. With a baseline affected by motion, the FFT artifacts can be completely corrected by using all the frequencies below 60 Hz as indicators of motion. With variable amplitudes, however, motion correction based only on 12 Hz removed some of the artifacts, but using additional frequencies created new artifacts. Unremovable artifacts sometimes occurred in this survey when the unstable probe stand had vibration frequencies of its own. Improved analysis methods and software are clearly needed to correct for probe motion in workplace measurements.

The most difficult problem with measuring magnetic field characteristics is their implications for evaluating workers' health risks. The Multiwave measurements do have clear implications for assessing adherence with the ELF magnetic field guidelines for acute health effects (ICNIRP, 1998; Physical Agents TLV Committee, 1999). Since these guidelines are derived from the induced current mechanism, they depend on the frequency spectrum as well as the ELF magnitude (Bowman, 1995), so the Multiwave can measure adherence more accurately than conventional ELF meters. How to measure guideline adherence with the Multiwave is the subject of current research.

The second issue is to link EMF hazard to possible

risks for cancer and other chronic diseases. Epidemiologic studies have found that risks of leukemia and brain cancer rise significantly with increasing TWA magnitudes of the ELF magnetic field (Portier and Wolfe, 1998; Kheifets *et al.*, 1999). But whether this exposure-response relationship is modified by other magnetic field characteristics still needs to be determined, as discussed above. Therefore, measurements of magnetic field characteristics are not useful for routine hazard evaluations at the present time, but could be very important if future studies find another metric of magnetic field exposure to be associated with disease. For such eventualities, a thorough workplace exposure assessment should clearly supplement the ELF magnitude monitors with the Multiwave or another waveform capture instrument.

### CONCLUSIONS

The Multiwave survey has provided a more detailed understanding of workplace magnetic fields and their sources than can be obtained by the usual measurements of ELF magnitudes with EMDEXs and similar monitors. These field characteristics measured by the Multiwave are important to the mechanisms postulated to explain biological effects, such as induced body currents, free radical production, and ion resonances (NIEHS, 1997; Bowman *et al.*, 2000). Since the characteristics measured in this survey vary greatly among the six workplaces, biological effects resulting from these postulated mechanisms could also vary in ways that can not be predicted by measurements of the ELF magnetic field magnitude. Exactly how these magnetic field characteristics affect worker health will require more theoretical, laboratory, and epidemiologic research on EMF biomechanisms and their impact on disease etiology.

While research continues regarding EMF mechanisms of action, a complete EMF exposure assessment should include measurements with the Multiwave or comparable instruments as a supplement to personal monitoring of the ELF magnitude. Our survey shows that spot measurements with the Multiwave II can adequately characterize industrial magnetic fields from 0 to 3000 Hz. However, the occasional difficulties in the Fourier analysis of workplace fields suggests that additional research on analyzing waveform data is needed to calculate magnetic field characteristics accurately and efficiently.

**Acknowledgements**—This survey was funded in part by the EMF RAPID program at the U.S. Department of Energy through Interagency Agreement #DE-AI01-94CE34008. We gratefully acknowledge the expert assistance received from Electric Research and Management, Inc. (ERM) throughout this project and from Jeremy Meredith (NIOSH) who wrote software for the Multiwave data analysis and graphics. William Gish (ERM) and Gary Johnson helped in identifying the sources of unusual frequency spectra.

### REFERENCES

- Blanchard, J. P. and Blackman, C. F. (1994) Clarification and application of an ion parametric resonance model for magnetic field interactions with biological systems. *Bioelectromagnetics* 15, 217–238.
- Bowman, J. D. (1995) Measuring multi-frequency magnetic fields for exposure assessments based on induced body currents. *Applied Occupational and Environmental Hygiene* 10, 628–634.
- Bowman, J. D. (1998) Calculating exposure metrics from three-axis waveform data In *Manual for Measuring Occupational Electric and Magnetic Field Exposures*, eds J. D. Bowman, M. A. Kelsch and W. T. Kaune, DHHS (NIOSH) Publication 98-154. National Institute for Occupational Safety and Health, Cincinnati, OH.
- Bowman, J. D., Thomas, D. C., London, S. J. and Peters, J. M. (1995) Hypothesis: The risk of childhood leukemia may be related to combinations of power-frequency and static magnetic fields. *Bioelectromagnetics* 16, 48–59.
- Bowman, J. D., Gailey, P. C., Gillette, L. and Lotz, W. G. (2000) *Proceedings of a Joint NIOSH/DOE Workshop on EMF Exposure Assessment and Epidemiology: Hypotheses, Metrics, and Measurements*, Publication PB 2000-101086. National Technical Information Service, Springfield, VA.
- Bracken, T. D. (1994) *Electric and Magnetic Fields in a Magnetic Resonance Imaging Facility: Measurements and Exposure Assessment Procedures*. Report to the National Institute for Occupational Safety and Health. Publication PB94-174489. National Technical Information Service, Springfield, VA.
- Conover, D. L., Murray, W. E., Foley, E. D., Lary, J. L. and Parr, W. H. (1980) Measurement of electric- and magnetic-field strengths from industrial radio-frequency (6–38 MHz) plastic sealers. *IEEE Proceedings* 68, 17–20.
- Deno, D. W. (1976) Transmission line fields. *IEEE Transactions on Power Apparatus and Systems* PAS-95, 1600–1611.
- Dietrich, F. M., Feero, W. E., Robertson, D. C. and Sicree, R. M. (1992) *Measurement of Power System Magnetic Fields by Waveform Capture*. EPRI Report TR-10006. Electric Power Research Institute, Palo Alto, CA.
- Dietrich, F. M. and Jacobs, W. L. (1999) *Survey and Assessment of Electric and Magnetic Field (EMF) Public Exposure in the Transportation Environment*. Electric Research, State College, PA (Report prepared for Department of Transportation under Contract No. DTRS-57-96-C-0073).
- Elmore, W. C. and Heald, M. A. (1969) In *Physics of Waves*, pp. 123–124. Dover, New York.
- ERM (Electric Research and Management) (1997) *Multiwave® System II User's Manual: Portable Magnetic Field Measurement Concept for Transient and Steady State Fields*, version 4.60T. Electric Research and Management, State College, PA.
- Gish, W.B., Dietrich, F.M., Rawson, M.T. and Feero, W.E. (1995) *Measurement of AC and DC magnetic fields in the presence of probe motion*. Unpublished report. Electric Research and Management, State College, PA.
- ICNIRP (International Commission on Non-Ionizing Radiation Protection) (1998) Guidelines for limiting exposure to time-varying electric, magnetic, and electromagnetic fields (up to 300 GHz). *Health Physics* 74, 494–522.
- Jackson, L. B. (1991) *Signals, Systems, and Transforms*. Addison-Wesley, Reading, MA (Chapter 4).
- Kheifets, L., Gilbert, E. S., Sussman, S. S., Guénel, P., Sahl, J. D., Savitz, D. A. and Thériault, G. (1999) Comparative analyses of the studies of magnetic fields and cancer in electric utility workers: Studies from France, Canada, and the United States. *Occupational and Environmental Medicine* 56, 567–574.
- Lednev, V. V. (1994) Interference with the vibrational energy sublevels of ions bound in calcium-binding proteins as the

- basis for the interaction of weak magnetic fields with biological systems In *On the Nature of Electromagnetic Field Interactions with Biological Systems*, ed. A. H. Frey, pp. 59-72. R.G. Landes, Austin, TX.
- Litovitz, T. A., Penafiel, M., Krause, D., Zhang, D. and Mullins, J. M. (1997) The role of temporal sensing in bioelectromagnetic effects. *Bioelectromagnetics* 18, 388-395.
- McKinlay, A. F. and Repacholi, M. H. (1999) Exposure metrics and dosimetry for EMF epidemiology (Proceedings of an International Workshop held at the National Radiological Protection Board). *Radiation Protection Dosimetry* 83, 1-194.
- Methner, M. M. and Bowman, J. D. (2000) Hazard surveillance for workplace magnetic fields: I. Walkthrough measurements of ELF fields. *Annals of Occupational Hygiene* 44, 603-614.
- National Geophysical Data Center (1998) Geomagnetic Field Synthesis Program (version 3.0). World Wide Web, <http://www.ngdc.noaa.gov/cgi-bin/seg/gmag/fidsnth1.pl><http://www.ngdc.noaa.gov/cgi-bin/seg/gmag/fidsnth1.pl>.
- NIEHS (National Institute of Environmental Health Sciences) (1997) *EMF Science Review Symposium: Breakout Group Reports on Theoretical Mechanisms and In Vitro Research Findings*. National Institute of Environmental Health Sciences, Research Triangle Park, NC (NIEHS/DOE EMF RAPID Program).
- Philips, K. L., Morandi, M. T., Oehme, D. and Cloutier, P. A. (1995) Occupational exposure to low frequency magnetic fields in health care facilities. *American Industrial Hygiene Association Journal* 56, 677-685.
- Physical Agents TLV Committee (1999) Sub-radiofrequency (30 kHz and below) magnetic fields In *1999 TLVs® and BEIs®: Threshold Limit Values for Chemical Substances and Physical Agents, Biological Exposure Indices*, pp. 143-144. American Conference of Governmental Industrial Hygienists, Cincinnati, OH.
- Portier, C. J. and Wolfe, M. S. eds. (1998) *Assessment of Health Effects from Exposure to Power-line Frequency Electric and Magnetic Fields*. NIEHS Working Group Report. National Institute of Environmental Health Sciences, Research Triangle Park, NC
- Rosner, B. (1995) One-sample *t* test In *Fundamentals of Biostatistics*, 4th edition, pp. 208-209. Duxbury Press, Belmont, CA.
- Sastre, A., Kavet, R., Ulrich, R.M., Guttman, J.L. and Weaver, J.C. (2000) Residential magnetic field transients induce transmembrane voltages that may exceed thermal noise. Submitted to *Bioelectromagnetics*.
- Valberg, P., Kaune, W. T. and Wilson, B. (1995) Designing EMF experiments: What is required to characterize 'exposure'?. *Bioelectromagnetics* 16, 396-406.
- Walleczek, J. (1995) Magnetokinetic effects on radical pairs: A paradigm for magnetic field interactions with biological systems at lower than thermal energy In *Electromagnetic Fields: Biological Interactions and Mechanisms*, ed. M. Blank, *Advances in Chemistry Series*, Vol. 250, pp. 395-420. American Chemical Society, Washington, DC.
- Wenzl, T. B. (1997) Estimating magnetic field exposures of rail maintenance workers. *American Industrial Hygiene Association Journal* 58, 667-671.